[redacted]

UNCLASSIFIED [redacted]

NACA

RESEARCH MEMORANDUM

for the

U. S. Air Force

ROCKET-MODEL MEASUREMENTS OF ZERO-LIFT DAMPING IN ROLL OF THE BELL MX-776 MISSILE AT MACH NUMBERS FROM 0.6 TO 1.56

By William M. Bland, Jr., and Paul E. Purser

Langley Aeronautical Laboratory
Langley Field, Va.

NATIONAL ADVISORY COMMITTEE
FOR AERONAUTICS
WASHINGTON

[redacted]

UNCLASSIFIED [redacted]

NACA RM SL54A13

NATIONAL ADVISORY COMMITTEE FOR AERONAUTICS

RESEARCH MEMORANDUM

for the

U. S. Air Force

ROCKET-MODEL MEASUREMENTS OF ZERO-LIFT DAMPING IN ROLL OF THE BELL MX-776 MISSILE AT MACH NUMBERS FROM 0.6 TO 1.56

By William M. Bland, Jr., and Paul E. Purser

SUMMARY

The zero-lift damping in roll of the Bell MX-776 missile has been measured by a sting-mounted rocket-model technique at Mach numbers from 0.6 to 1.56.

The damping-in-roll data, in general, show no unusual variation with Mach number. Aileron rolling-moment effectiveness derived from these data and previously obtained rolling-effectiveness data appear reasonable.

INTRODUCTION

The NACA is conducting an investigation of the aileron control characteristics of the Bell Aircraft Company MX-776 missile at the request of the U. S. Air Force. A study of aileron rolling effectiveness and drag of rocket-powered models of the MX-776 is presented in reference 1. As a part of this investigation the Langley Pilotless Aircraft Research Division has measured the zero-lift damping in roll of a 1/24-scale model of the MX-776 at Mach numbers from 0.6 to 1.56 using the sting-mounted rocket-model technique of reference 2. The flight was made at the Langley Pilotless Aircraft Research Station, Wallops Island, Va.

This paper presents these damping-in-roll data and presents aileron rolling-moment effectiveness data derived from these damping-in-roll data and the aileron rolling-effectiveness data of reference 1.

SYMBOLS

C_l	rolling-moment coefficient, L/qSb
L	rolling moment, lb-ft
q	dynamic pressure, lb/sq ft
S	total included area of rear horizontal wing, sq ft
b	span of rear horizontal wing, ft
c	chord, ft
$\frac{pb}{2V}$	wing-tip helix angle, radians
p	rate of roll, radians/sec
V	velocity, fps

$$C_{l_p} = \frac{dC_l}{d\left(\frac{pb}{2V}\right)}$$

$$C_{l_{\delta_a}} = \frac{dC_l}{d\delta_a}$$

δ_a	total aileron deflection, deg
i_w	section wing incidence, deg
M	Mach number
R	Reynolds number, based on mean aerodynamic chord of rear horizontal wing

MODEL

The 1/24-scale model of the MX-776 which was built at Langley with a dural body and steel fins is shown in figures 1 and 2. The model was highly polished, the frosted appearance evident in figure 2 was a

protective coating which was removed before firing. The model was mounted on a sting at the nose of the carrier vehicle as shown in figure 3.

Preflight measurements of the model showed the various wing panels to have small misalinements, relative to the model center line, varying from 0.21° nose down to 0.18° nose up. The root-mean-square misalinement angle was 0.088°. The measured values of misalinement angle and other wing geometric characteristics are listed in tables I and II.

TEST PROCEDURE

The model was tested using the sting-mount technique described in reference 2. The procedure consisted of mounting the model at zero angle of attack and zero angle of sideslip on a torsion balance at the nose of the rocket carrier vehicle shown in figure 3. The fins on the carrier vehicle were twisted to cause the combination to roll continuously as the vehicle accelerated to maximum speed and decelerated, in coasting flight, after burnout of the rocket motor.

During the flight the model was tracked with CW Doppler and modified SCR-584 radar sets to provide velocity and altitude data. The torsion-balance data were telemetered to ground receiving stations and rolling-velocity data were obtained from the telemeter transmitter signal by the method described in reference 3. Atmospheric data were obtained from a radiosonde released immediately after the model flight.

DATA REDUCTION AND ACCURACY

Data Reduction

The telemetered data from the torsion balance and the rolling-velocity data were converted to rolling-moment coefficients and wing-tip helix angles as functions of time and Mach number. Assuming linearity of C_l with $\frac{pb}{2V}$, C_{l_p} was obtained from the relation

$$C_{l_p} = \frac{C_l}{\frac{pb}{2V}}$$

Calculations employing strip theory indicated that previously noted misalinements present in the model surfaces could cause the measured values of C_{l_p} to be low by not more than 5 percent. Accordingly, the C_{l_p} values presented have been increased by this amount.

Data Accuracy

The accuracy of the data, based on previous experience with the instrumentation is estimated to be within the following limits:

M	ΔC_{l_p}	ΔM
1.5	±0.012	±0.01
1.0	±.025	±.01
.6	±.040	±.01

Variations with Mach number are believed to be more accurate than indicated by the above limits.

RESULTS AND DISCUSSION

Damping in Roll

The values of C_{l_p} obtained from this flight are shown in figure 4 along with the test Reynolds number for the Mach number range from 0.6 to 1.56. The test $\frac{pb}{2V}$ varied from 0.034 to 0.037 over the Mach number range.

The data show no extreme variations of C_{l_p} with Mach number although the general level of C_{l_p} changes from about 0.35 at $M < 0.8$ to 0.42 at supersonic speeds. Also shown in figure 4 are linear-theory values of C_{l_p} calculated from reference 4 corrected for wing-body interference by the method of reference 5. No allowance was made for wing-to-wing interference or downwash. These effects probably account for the major part of the difference shown between calculations and experiment in figure 4.

Aileron Rolling-Moment Effectiveness

Utilizing the damping-in-roll data of figure 4 and the aileron rolling-effectiveness data of reference 1 the relation

$$C_{l_{\delta_a}} = -\frac{\frac{pb}{2V}}{\delta_a} C_{l_p}$$

was used to obtain the aileron rolling-moment effectiveness $C_{l_{\delta_a}}$ shown in figure 5. Note that $C_{l_{\delta_a}}$ is based on total aileron deflection and on total area and span of the rear horizontal wing.

Shown for comparison in figure 5 are values of $C_{l_{\delta_a}}$ for the MX-776 from wind-tunnel tests at $M = 1.56$ (ref. 6). The flight data appear slightly high compared to the tunnel data at supersonic speeds. The differences at transonic speeds between the data for the various δ_a values may be a result of nonlinear control effectiveness or of differences in the detail geometry of the three rolling-effectiveness models.

CONCLUDING REMARKS

Damping-in-roll data measured in a rocket-model flight test of the MX-776, in general, show no unusual trends with Mach number. Aileron rolling-moment effectiveness derived from these data and previously obtained rolling-effectiveness tests appear reasonable in trend and magnitude.

Langley Aeronautical Laboratory,
National Advisory Committee for Aeronautics,
Langley Field, Va., December 31, 1953.

William M. Bland, Jr.
Aeronautical Research Scientist

Paul E. Purser
Aeronautical Research Scientist

Approved:

Joseph A. Shortal
Chief of Pilotless Aircraft Research Division

lso

[redacted]

REFERENCES

1. Stevens, Joseph E.: Preliminary Results of a Flight Investigation of 1/6-Scale Rocket-Powered Models of the Bell MX-776 To Determine Aileron Rolling Effectiveness and Total Drag. NACA RM SL51D27, U. S. Air Force, 1951.

2. Bland, William M., Jr., and Sandahl, Carl A.: A Technique Utilizing Rocket-Propelled Test Vehicles for the Measurement of the Damping in Roll of Sting-Mounted Models and Some Initial Results for Delta and Unswept Tapered Wings. NACA RM L50D24, 1950.

3. Harris, Orville R.: Determination of the Rate of Roll of Pilotless Aircraft Research Models by Means of Polarized Radio Waves. NACA TN 2023, 1950.

4. Piland, Robert O.: Summary of the Theoretical Lift, Damping-in-Roll, and Center-of-Pressure Characteristics of Various Wing Plan Forms at Supersonic Speeds. NACA TN 1977, 1949.

5. Tucker, Warren A., and Piland, Robert O.: Estimation of the Damping in Roll of Supersonic-Leading-Edge Wing-Body Combinations. NACA TN 2151, 1950.

6. Darling, J. A., and DeMeritte, F. J.: Static Stability Measurements on Rascal Missile (MX-776) at Mach Number 1.56. NAVORD Rep. 2362, U. S. Naval Ord. Lab., White Oak, Md., June 11, 1952.

TABLE I.- MEASURED FIN SETTINGS AND THICKNESS RATIOS

Fin	Spanwise distance, in. from body center line to measuring station	i_w, deg[a]	Thickness ratio
Rear horizontal, right	1.5 3.0 4.0	0.050 .010 .130	0.058 .052 .041
Rear horizontal, left	1.5 3.0 4.0	.014 -.008 .032	.059 .053 .043
Rear vertical, top	1.5 2.0 3.0	.050 .185 -.006	.048 .046 .036
Rear vertical, bottom	1.5 2.0 3.0	.080 -.054 .016	.047 .045 .034
Forward horizontal, right	1.5 2.0 2.5	.013 .095 .013	.045 .043 .036
Forward horizontal, left	1.5 2.0 2.5	.040 .049 .039	.046 .042 .037
Forward vertical, top	1.0 1.5	-.214 -.158	.044 .035
Forward vertical, bottom	1.0 1.5	.090 .095	.046 .036

[a]Positive values of i_w tend to apply a clockwise moment to the model when viewed from the rear. For example $i_w = +0.010^\circ$ on right rear horizontal fin is a leading-edge-down setting.

TABLE II.- MEASURED GEOMETRIC CHARACTERISTICS

[Fuselage: overall length, 16.00 in.; maximum diameter, 2.00 in.]

	Rear horizontal fins	Rear vertical fins	Forward horizontal fins	Forward vertical fins
Aspect Ratio	3.0	3.2	3.3	3.9
Taper ratio, $\frac{\text{Tip chord}}{\text{Root chord}}$	0.26	0.26	0.25	0.21
Total span, in.	8.35	6.25	5.77	3.33
Total area, sq in.	23.33	12.25	10.05	2.80
Sweep, 0.75 chord, deg[a]	0	0	0	0
Hinge-line location, percent chord[a]	75.0	-----	-----	----
Airfoil Section[a]	(b)	(d)	(c)	(d)

[a]Design value.

[b]Symetrical circular arc with full-slab behind 75-percent chord.

[c]Symetrical circular arc with half-slab behind 75-percent chord.

[d]Symetrical circular arc.

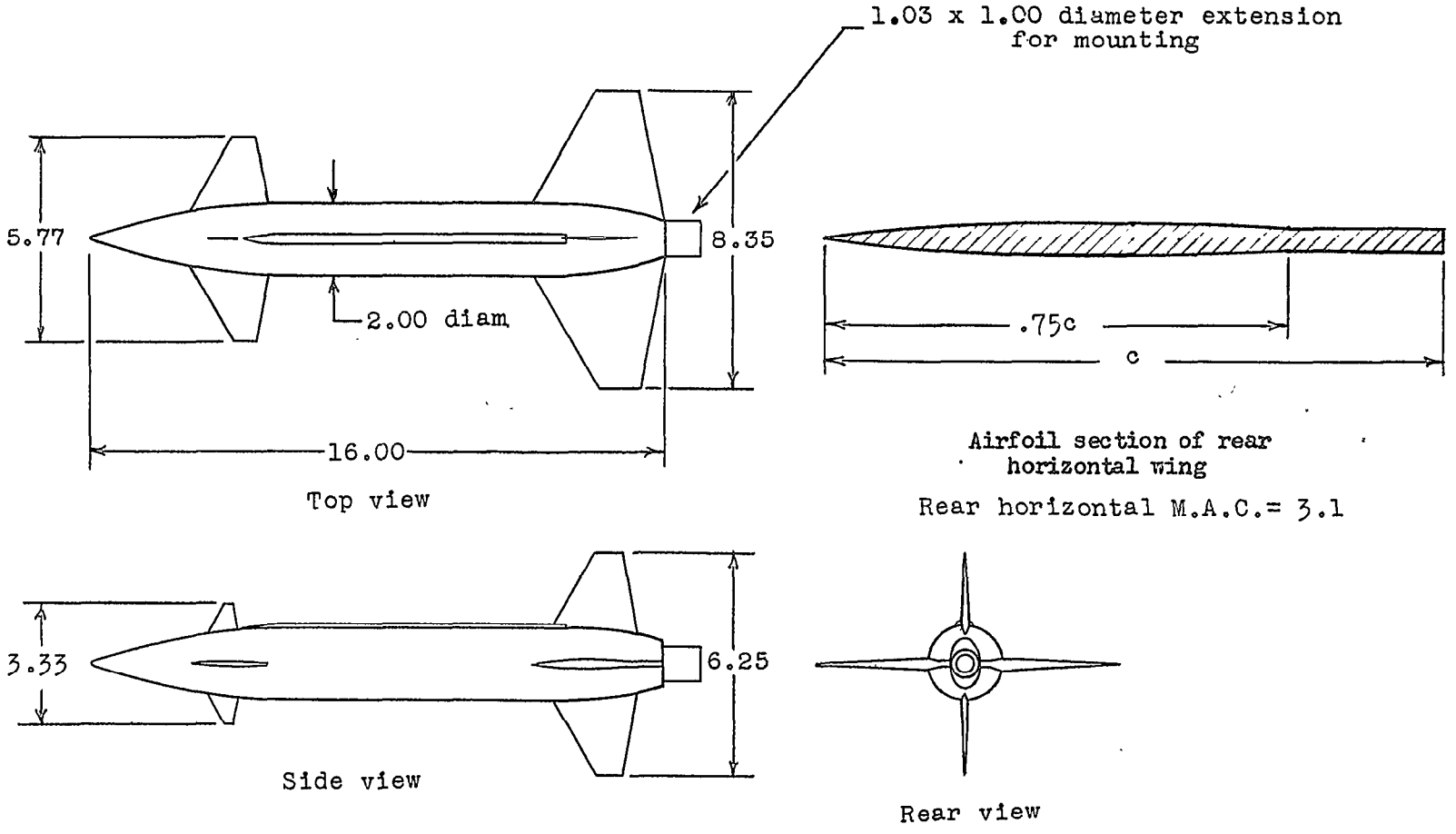

Figure 1.- General arrangement of $\frac{1}{24}$-scale model of Bell MX-776 missile.
All dimensions in inches.

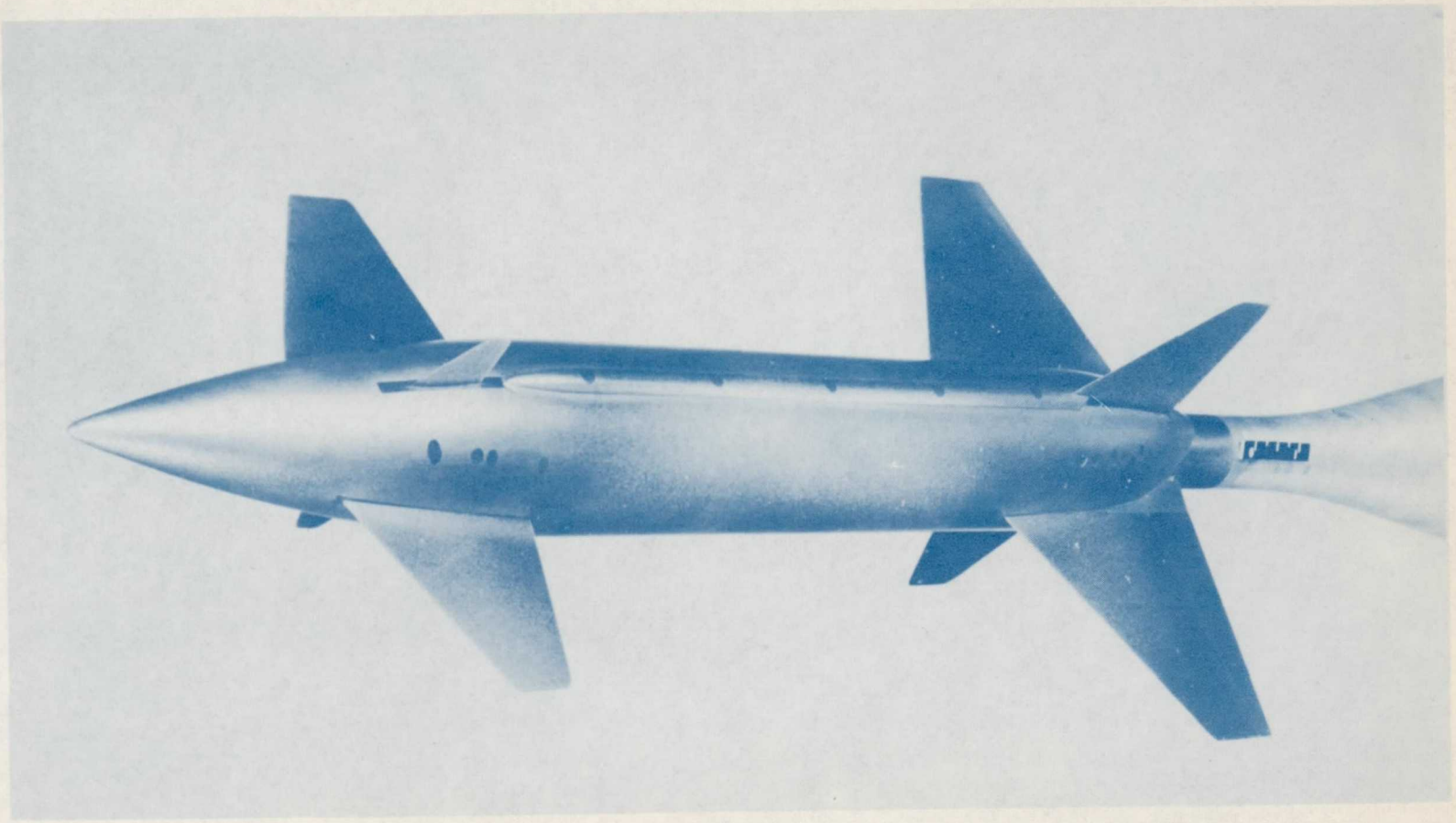

L-76768

Figure 2.- The $\frac{1}{24}$-scale model of Bell MX-776 attached to forward section of rocket vehicle.

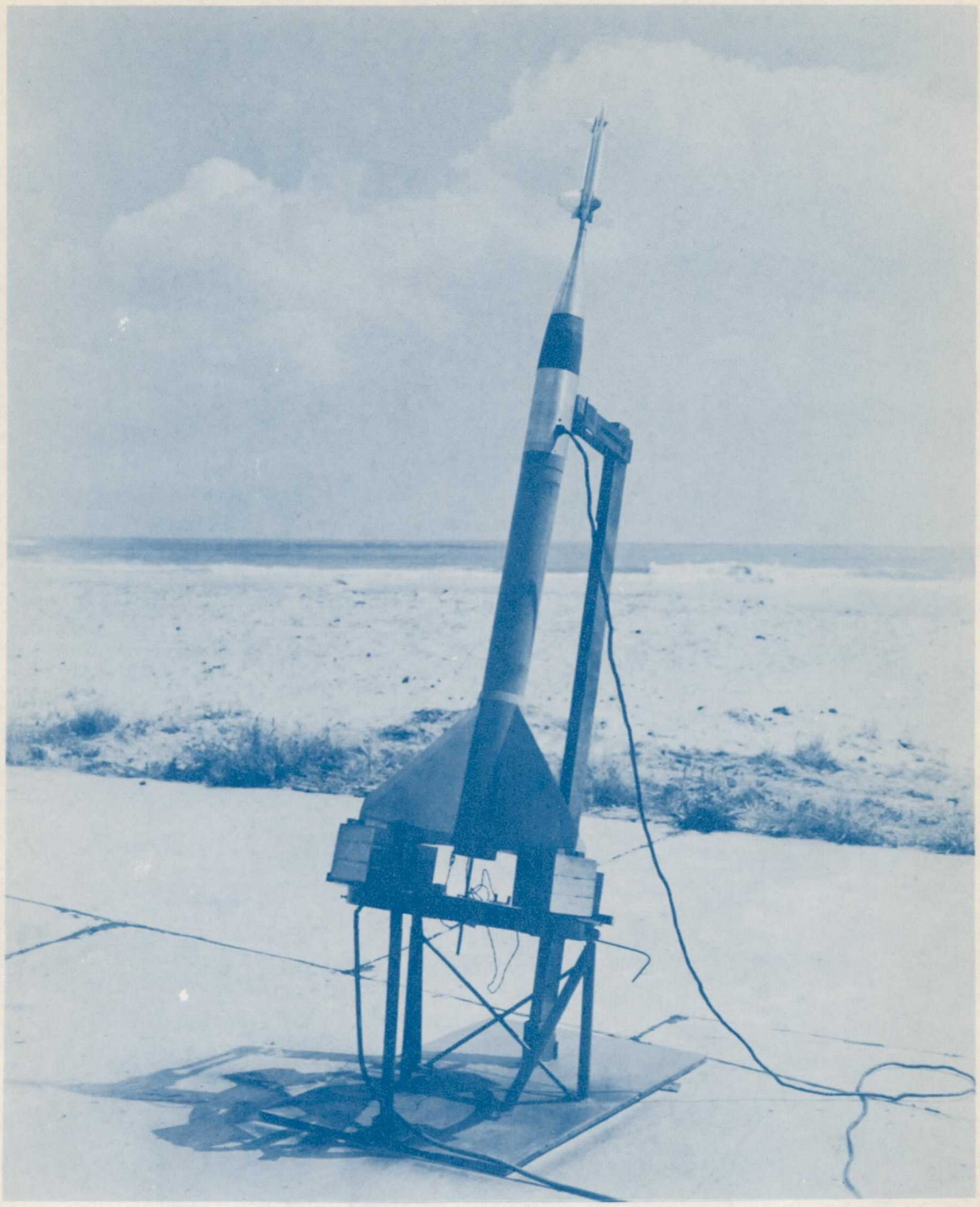

L-76820.1

Figure 3.- Model and rocket vehicle on launcher.

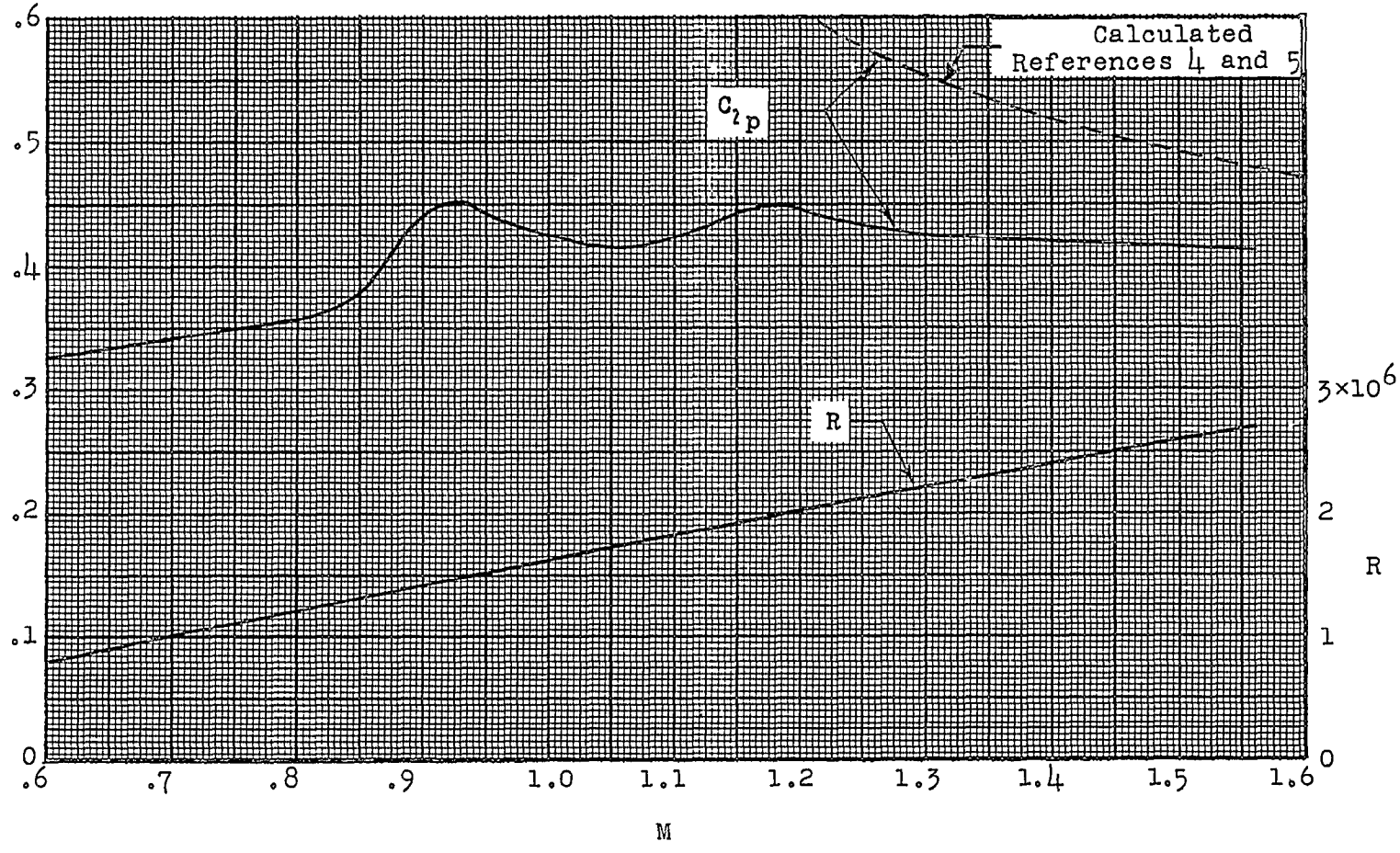

Figure 4.- Variation of damping-in-roll coefficient and Reynolds number with Mach number.

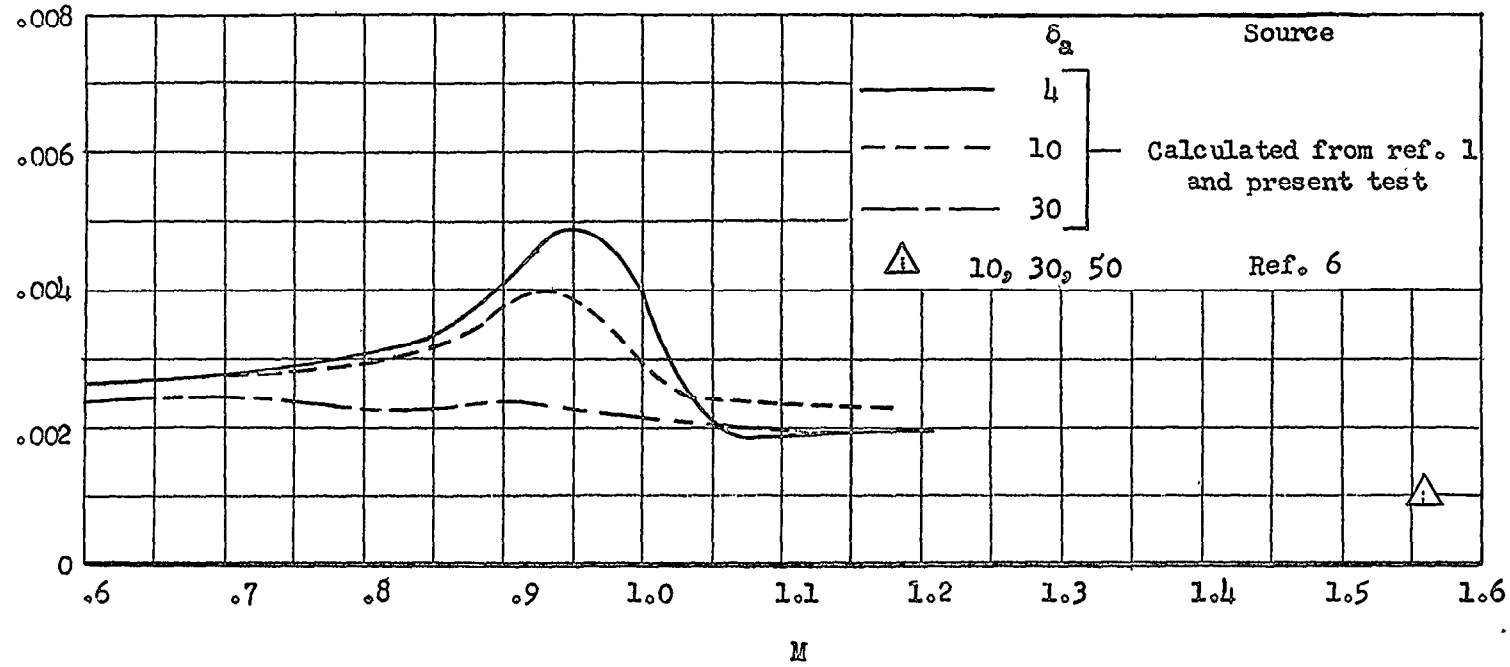

Figure 5.- Variation of aileron rolling-moment coefficient with Mach number.